

Model Catalyst Studies on Vanadia Particles Deposited onto a Thin-Film Alumina Support. 2. Interaction with Carbon Monoxide

Norbert Magg, Javier B. Giorgi,[‡] Ayman Hammoudeh,[§] Thomas Schroeder,[‡]
Marcus Bäumer,[#] and Hans-Joachim Freund*

Fritz-Haber-Institut der Max-Planck-Gesellschaft, Faradayweg 4-6, D-14195 Berlin, Germany

The interaction of CO molecules with a model catalyst system formed by alumina-supported vanadia particles was studied utilizing infrared (IR) spectroscopy. A thin, well-ordered alumina film grown on the NiAl(110) alloy surface was used as a support oxide. The structural characterization of this model system has been performed previously by applying scanning tunneling microscopy, X-ray photoelectron spectroscopy, and IR spectroscopy. Exposure to CO at 90 K results in a complex adsorption behavior as a function of vanadia particle size. At high vanadia coverages, only one CO species can be detected that interacts with vanadyl groups (V=O) present at the surface of the particles. At lower coverages, however, three further species were observed. Their existence seems to be correlated with either defect sites or with special sites provided at the vanadia–alumina interface. Furthermore, particles in this coverage regime are capable of adsorbing a maximum amount of CO molecules. Regarding the reactivity of our model system, we found only molecular desorption of CO upon thermal treatment. However, exposing the CO covered particles to low-energy electrons renders a reaction possible. A portion of the adsorbed CO gets oxidized to CO₂ via a redox mechanism, i.e., by a transfer of lattice oxygen. According to our experiments, the vanadyl oxygen does not seem to be the species that is consumed during the course of the reaction.

1. Introduction

Submonolayer to monolayer quantities of oxide-supported vanadium oxides are known to be active in a variety of industrially applied oxidation and reduction reactions.^{1,2} Consequently, many past investigations have attempted to correlate structural properties of supported vanadia particles with their reaction behavior. However, there are still many open questions, in regard to, for example, the role of the supporting oxide or the role of vanadyl groups, which are always present in technical catalysts.^{1,2} To contribute to these issues, we have prepared a model catalyst system under ultrahigh vacuum (UHV) conditions that exhibits a reduced complexity, thus rendering a more-detailed structural characterization possible. The results of our investigations on this topic have been published recently in another issue of this journal³ and shall be therefore just briefly repeated here.

The model system is prepared via the evaporation of vanadium onto a thin, well-ordered alumina film that can be grown on the NiAl(110) surface. During evaporation, the sample is kept at a temperature of 300 K and in an oxygen ambient of 1×10^{-7} mbar O₂. This procedure leads to the growth of small, roundish particles with diameters in the range of 20–30 Å. A strong interaction of vanadium with the alumina support, as well as with the oxygen ambient results in a comparatively high particle number density of $\sim 2 \times 10^{13}$ particles/cm² and partial incorporation of the particles into the alumina film. The average

oxidation state of vanadium is close to +3; however, the structure of the particles is quite different from that of V₂O₃. As evidenced by infrared (IR) spectroscopy, surface-localized vanadyl groups (V=O) and interface-localized species, which comprise a combined vibration of V, O, and Al ions, are present in the system.

In this second paper, we focus on the interaction of our model catalyst system with carbon monoxide (CO) and the question of how this interaction is dependent on the structural properties.

2. Experimental Section

All CO adsorption and reaction experiments were performed in the multichamber UHV system that was already described previously.³ This system is operated at a base pressure of $< 2 \times 10^{-10}$ mbar and is equipped with facilities to perform scanning tunneling microscopy (STM), X-ray photoelectron spectroscopy (XPS), and IR spectroscopy. Because, essentially, the latter technique was used to obtain the results presented in the following, we refer to our previous publication³ for a description of the STM and XPS setup. IR spectra were acquired with a Fourier transform infrared (FTIR) spectrometer (Bruker model IFS 66v/S). P-polarized light was coupled into the UHV chamber via viton sealed KBr windows and reflected from the sample surface at an angle of 84°. Spectra were recorded using a liquid-nitrogen-cooled MCT detector operating in the mid-IR region at frequencies of > 600 cm⁻¹. Typically, 4000 scans were accumulated for the reference spectra, i.e., for the clean NiAl substrate and the clean vanadia particles, and 1000 scans for the CO covered system. Spectral resolution after apodization was 3.3 cm⁻¹. For the following, it is important to note that the metal surface selection rule applies for the system that is discussed here, because of the limited thickness of the alumina film and the metal substrate underneath it. As a result, only structures that exhibit a nonzero component of the dynamic

* Author to whom correspondence should be addressed. E-mail: freund@fhi-berlin.mpg.de.

[‡] Present address: University of Ottawa, Ottawa, Canada.

[§] Now with Yarmouk University, Irbid, Jordan.

[‡] Present address: European Synchrotron Radiation Facility, Grenoble, France.

[#] Present address: Universität Bremen, Institut für Angewandte und Physikalische Chemie, Bremen, Germany.

dipole moment perpendicular to the NiAl substrate can be observed in the IR spectra.

The preparation of the model catalyst system was conducted in two steps, comprising the growth of the alumina thin-film support and the deposition of vanadia particles. In a first step, a sputter-cleaned NiAl(110) surface that was kept at a temperature of 550 K was exposed to ~ 3000 L of O_2 ($1 \text{ L} = 10^{-6}$ Torr s) and subsequently annealed at ~ 1100 K.⁴ Usually, two oxidation/annealing cycles were employed to ensure complete oxidation of the NiAl surface. This results in a well-ordered alumina film ~ 5 Å thick.^{4–6} After the preparation, the quality of the oxide film was checked by STM and low-energy electron diffraction (LEED). In a second step, vanadium ($>99.8\%$, Goodfellow) was deposited by means of an electron-beam evaporator (model EFM3T, Focus) in an oxygen ambient of 1×10^{-7} mbar O_2 . During vanadium evaporation, the sample was held on a retarding potential, to prevent V ions from being accelerated toward the sample. The deposition rate of 0.36 monolayers per minute (0.36 ML/min) was determined by means of a quartz crystal microbalance and counterchecked by two-dimensional submonolayer growth on NiAl(110) and subsequent STM measurements. Because the stoichiometry and morphology of the prepared vanadia particles may change with increasing vanadium loading, all coverages cited are expressed in terms of the number of monolayers of vanadium metal deposited. One monolayer of vanadium (1 MLV) was calculated on the basis of the interlayer distance between the close-packed (110) planes of bulk vanadium of 2.14 Å, which corresponds to 1.54×10^{15} atoms/cm².

The adsorption of CO ($>99.997\%$, AGA) was conducted directly in the IR cell, utilizing a gasdoser system (pinhole doser) and with the sample being kept at ~ 90 K. To remove any contaminants from the CO gas feed (e.g., nickel carbonyls present in the gas cylinder), we passed the CO gas through a cooling trap that was operated at liquid nitrogen temperature. Furthermore, it is important to note that, at a sample temperature of 90 K, CO does not adsorb on the clean alumina substrate. Consequently, all CO signals observed in our IR spectra are due to the presence of the vanadia overlayer.

3. Results

The results presented in the following discussion are grouped into three sections. The first section involves the low-temperature adsorption behavior of CO on the vanadia particles as a function of particle size, whereas the second section concentrates on the interaction between adsorbed CO and oxide vibrations of the vanadia overlayer. The last section describes the conditions under which CO can be oxidized to CO_2 .

3.1. CO Adsorption. In Figure 1, IR spectra are presented for CO-saturated vanadia particles. The three spectra shown are representative for three different regions into which the CO adsorption behavior can be subdivided, as a function of vanadia particle size.⁷ An analysis of an entire series of CO saturation spectra is shown in Figure 2. The way in which the different CO peaks develop, as a function of vanadium coverage, can be used to define the above-mentioned three regions of CO adsorption as follows: (i) “low coverage”, 0–0.15 MLV (0–10 V atoms per particle); (ii) “medium coverage”, 0.15–0.6 MLV (10–50 V atoms per particle); and (iii) “high coverage”, 0.6–2.0 MLV (50–180 V atoms per particle).

Altogether, four different CO peaks (denoted as P0–P3) can be distinguished, among which P1 is clearly the dominating CO peak. It belongs to the most intense feature and is the only one present in the entire coverage regime. As a function of increasing

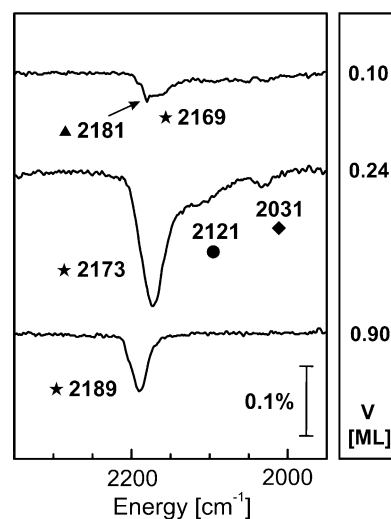


Figure 1. IR spectra of CO-saturated vanadia particles. Their size is indicated on the right side, in terms of the number of monolayers (ML) of vanadium metal deposited. Symbols plotted next to the given frequency values refer to those used in Figure 2a. Experimental conditions: CO exposure and data acquisition were carried out at 90 K; spectra were referenced to the corresponding clean vanadia particles.

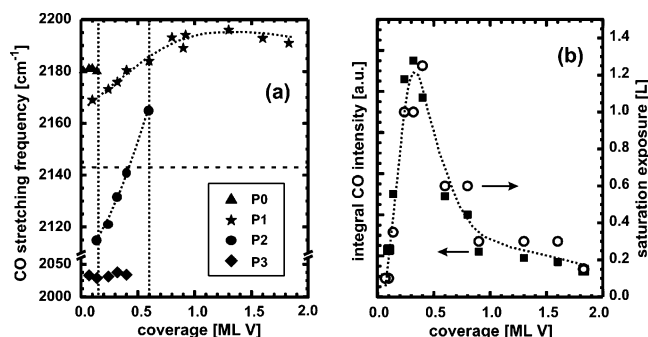


Figure 2. Analysis of an entire series of IR spectra of CO-saturated vanadia particles. Experimental conditions are as in Figure 1. (a) CO stretching frequency plotted for the four species P0–P3, as a function of vanadium coverage; the vertical dotted lines indicate the division into three coverage regimes, as discussed in the text, whereas the horizontal dashed line marks the stretching frequency of CO in the gas phase (2143 cm^{-1}). (b) Total peak area, as calculated by integration over all CO peaks (filled square symbols), and CO exposure required to saturate the vanadia particles (open circular symbols).

coverage, its width decreases from 40 to 20 cm^{-1} , whereas its position shifts from 2169 cm^{-1} up to 2196 cm^{-1} . Hence, peak P1 is blue-shifted with respect to the gas-phase value (2143 cm^{-1}), as expected for CO that is adsorbed on oxide surfaces.^{8–12} According to theoretical calculations on MgO and NiO ,¹³ the bonding with CO is almost entirely electrostatic in nature, i.e., no significant σ donation or π back-donation contributions are involved, even in the case of transition-metal oxides with partially filled d-shells. Instead, the observed blue-shift is essentially due to the so-called wall effect, i.e., the Pauli repulsion between carbon lone-pair electrons and the surface charge distribution. Consistent with that statement, blue-shifted CO signals were found on well-ordered V_2O_3 films^{14,15} and on reduced vanadia catalysts for which the following classification was published:¹⁶ V^{3+} , 2178 – 2190 cm^{-1} ; and V^{4+} , 2180 – 2212 cm^{-1} . Note that, in contrast to the system under discussion, only a small frequency shift (of approximately $+7 \text{ cm}^{-1}$) was observed as a function of the vanadium loading for CO adsorption on alumina-supported vanadia catalysts prepared by wet impregnation techniques.¹⁷

Unlike the P1 species, the P2 and P3 peaks are visible only in the medium- or low-coverage regime and are found to be red-shifted with respect to the gas-phase value, indicating a non-negligible contribution of π -back-donation electrons. The corresponding adsorption sites are, therefore, likely to involve defect sites. In fact, for the P3 species, we were able to show that its intensity is correlated to the number of steps on the alumina support. This was achieved by replacing the NiAl crystal that is usually used for the alumina film growth by another NiAl crystal where the step density was a factor of 5 greater. In this case, the intensity of the P3 peak also was 5 times larger than that usually observed. It should be emphasized in this context that the alumina steps themselves cannot be directly responsible for the P3 species, because CO does not adsorb onto alumina at the temperature applied. Instead, the vanadia particles grown at such alumina steps must exhibit a special type of adsorption site, which leads to the appearance of the P3 peak. The P0 species, finally, exists only in the low-coverage range and is characterized by a very narrow peak width of $\sim 6\text{ cm}^{-1}$ and a position of $\sim 2180\text{ cm}^{-1}$.

So far, we have focused our discussion on the frequency behavior of the adsorbed CO species. However, the absorption intensity that is due to CO stretching vibrations also shows an interesting dependence on the vanadia particle size: for a coverage of $\sim 0.3\text{ MLV}$, the IR intensity gets maximal, reaching a value that is ~ 5 times larger than that obtained in the high-coverage regime. This is already visible in Figure 1 and is shown in more detail in Figure 2b. There, the CO peak intensity, integrated over all peaks, is plotted as a function of the vanadium coverage. It seems that particles in the medium-coverage regime (i.e., $\sim 0.3\text{ MLV}$, or 25 V atoms per particle) are capable of adsorbing a maximum amount of CO. However, only components of the CO dynamic dipole moment that are oriented perpendicular to the metal substrate contribute to the measured IR signal;¹⁸ therefore, it is conceivable that the observed intensity maximum is due to a vanadium-coverage-dependent change in CO orientation with respect to the substrate surface. To exclude this possibility, we also have plotted, in the same graphic, the amount of CO that had to be supplied to saturate the vanadia particles. Obviously, the two curves follow exactly the same trend, i.e., a high absorption signal is correlated to a large CO saturation dosage and vice versa. Also, an increasing dipole–dipole interaction between neighboring CO molecules, as a function of vanadium coverage, can be excluded as an explanation for the observed intensity decline:¹⁸ the P1 species, which clearly dominates the intensity behavior, shows only a very small frequency shift as a function of increasing CO exposure, being -3 cm^{-1} for vanadium coverages of $\sim 0.3\text{ MLV}$ and $\sim 0\text{ cm}^{-1}$ at high vanadium coverages. This proves that dipole–dipole interactions are negligible in our case. Further evidence for the idea of a particle-size-dependent CO adsorption capability comes from the observation that the interaction of CO with $\text{V}=\text{O}$ also becomes maximal at $\sim 0.3\text{ MLV}$ (see section 3.2). Interestingly, the CO desorption temperature of the P1 species (more details are given in section 3.3) also was found to follow a similar trend, as a function of the vanadium coverage: 140 K (low coverage), 175 K (medium coverage), and 140 K (high coverage).

Finally, we must mention that the overall CO absorption intensity measured on our particles is quite low, as compared to other systems. Although the peak height of the most intensive species (P1) ranges between $\sim 0.05\%$ (for low and large vanadium coverages) and $\sim 0.25\%$ (for medium vanadium coverage), considerably higher signals were found on metal

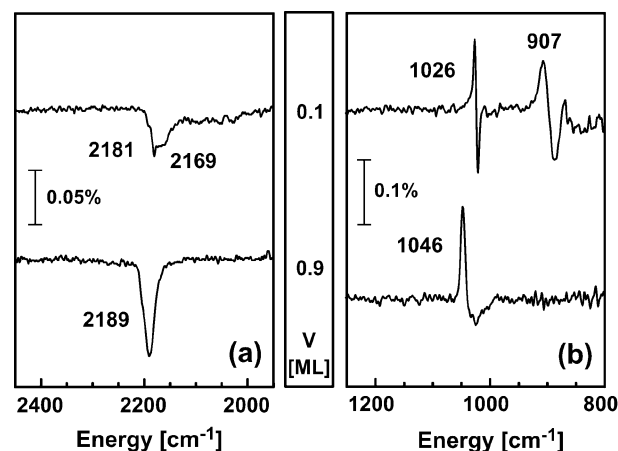


Figure 3. Set of IR spectra of CO-saturated vanadia particles of two different coverages (0.1 and 0.9 MLV): (a) region of CO stretching vibrations and (b) region of oxide vibrations. Experimental conditions are as in Figure 1.

particle systems that had been prepared on the same alumina support. On iridium particles,^{19,20} for example, the following peak heights were found: $\sim 0.25\%$ (low iridium coverage) and $\sim 4\%$ (large iridium coverage). The same is true for CO on metal single crystals, e.g., on Ir(111), where a peak height of $\sim 2\%$ was reported.²¹

There are two possible scenarios that could explain why the absorption intensity for our CO-saturated vanadia particles is that low. One possibility could simply be that only a small number of CO adsorption sites is present in our system; the other possibility to explain the low intensity is a CO adsorption geometry in which the molecules are oriented almost parallel to the NiAl substrate. Angle-resolved ultraviolet photoelectron spectroscopy (ARUPS) experiments revealed that the latter scenario is responsible for the low IR absorption intensity (peak height of $\sim 0.5\%$) measured for CO adsorption on a well-ordered $\text{Cr}_2\text{O}_3(0001)$ film grown on Cr(110), a system that has been studied intensively in our group.^{22,23} Note that, in this case, the CO frequency shifted by approximately -8 cm^{-1} , as a function of CO exposure. Analogous ARUPS results were obtained for CO adsorption on well-ordered, isostructural V_2O_3 films,^{14,15} so that a similar adsorption geometry also could apply in our case. However, our small IR signal intensities cannot be explained on the basis of a strongly tilted adsorbate geometry only, because XPS measurements (Al K α , 150 eV pass energy) on CO-saturated vanadia particles (0.4 MLV) revealed only a very small C 1s signal. The small CO-coverage-dependent frequency shift (less than or equal to -3 cm^{-1}) points in the same direction.

Possibly, the termination of our particles with vanadyl groups has a strong impact on their CO adsorption capability. This is suggested by recent experiments on thick, well-ordered V_2O_3 films that could be prepared either with or without terminating $\text{V}=\text{O}$ groups. In the latter case, ARUPS evidenced a significantly larger amount of CO that could be adsorbed on the film.^{14,15}

3.2. Interaction of CO with Oxide Vibrations. So far, only the frequency regime of $2000\text{--}2200\text{ cm}^{-1}$ (i.e., the region of CO stretching vibrations) has been discussed. However, there are also signals to be observed at lower frequencies that are typical for the oxide vibrations of our system ($700\text{--}1100\text{ cm}^{-1}$) already discussed previously.³ In Figure 3, IR spectra of CO-saturated particles (0.1 and 0.9 MLV) are presented which are split into the region of (a) CO stretching and (b) oxide vibrations.

In this latter region, signals can be observed that point in the direction opposite to the usual absorption peaks; therefore, these signals will be called “anti-peaks” in the following discussion. Their development as a function of CO exposure proceeds entirely synchronously to that of the CO stretching signals (i.e., anti-peaks increase (decrease) as long as CO peaks increase (decrease) and also saturate after the same CO exposure) and was proven to be reproducible by many different experiments.

To understand what is causing these anti-peaks to appear, one must know that the IR spectra shown in Figure 3 are measured with respect to the clean vanadia particles.²⁴ Since CO adsorption can be conducted directly in the IR cell—without the need to change the sample position—spectra with a very well-defined, horizontal baseline can be obtained that way. As will become clear in the following, this allows us to observe, unambiguously, small frequency and intensity changes of vanadium oxide vibrations that are induced by their interaction with CO molecules adsorbed on the particles. Because of the above-described relative spectrum acquisition, these changes manifest themselves as sharp anti-peak features that are easy to observe. To make the changes that result in these anti-peaks visible, one must divide both the single-channel spectra of the clean particles and that of the CO-covered particles by a single-channel spectrum of the NiAl metal substrate, which was measured beforehand, during the alumina film preparation. Note that, in this case, the baseline of the spectra is less well-defined, making the use of baseline correction methods necessary.

Panels a and c of Figure 4 show the result of such a reference change performed for the high- and low-coverage preparation presented in Figure 3. The spectra plotted at the top are just a copy of those from Figure 3b, whereas the spectra at the bottom are those referenced to NiAl. Obviously, the CO-induced changes are very small; nevertheless, they are reproducible, as already stressed previously. For a better understanding, the interesting parts of the spectra are presented as close-ups in Figure 4b and 4d, respectively, and shall be discussed in the following.

For the 0.9 MLV preparation, only one anti-peak is found, at a frequency of 1046 cm^{-1} . Consequently, only the region of vanadyl vibrations is modified upon CO adsorption, as can be observed in Figure 4a. The close-up reveals that the interaction of CO with vanadyl groups causes a shift of the V=O stretching frequency by approximately -2 cm^{-1} , accompanied by a decrease in the intensity of the V=O band. This proves that the V=O groups present in our system are, as suggested previously,³ localized at the surface of the vanadia particles, where they are accessible for adsorbed CO. Similar observations were reported in the literature on supported vanadia catalysts for the interaction of V=O with CO^{16,25} but also with other molecules, such as 2-propanol,²⁶ for instance.

It should be mentioned that the observed interaction between the CO molecules and the V=O groups is mutual, in the sense that not only the adsorbed CO molecules influence the V=O vibration frequency inducing a *red-shift* but also vice versa. Unfortunately, this latter case cannot be studied as easily as the CO-induced influence, because there is no simple way to change the V=O coverage. However, we have a set of experiments where vanadia particles of a certain size had been prepared twice but where the number of V=O groups present at the surface—judged from the corresponding IR intensity, assuming a fixed adsorbate geometry—happened to differ by a factor of ~ 2.5 . In the case of the high V=O density preparation, the observed CO peak P1 was found to be *blue-shifted*, by $\sim 10 \text{ cm}^{-1}$.

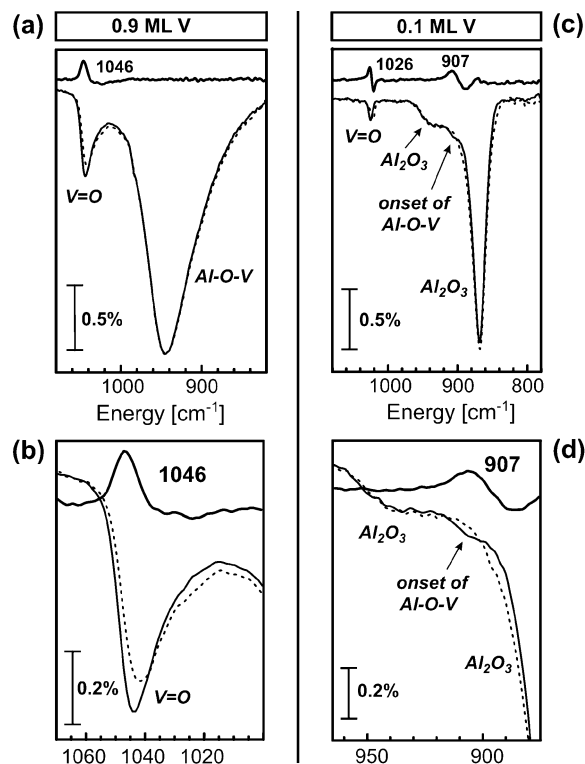


Figure 4. Set of IR spectra of CO-saturated vanadia particles of two different coverages (0.1 and 0.9 MLV): (a) 0.9 MLV, frequency region of oxide vibrations; (b) close-up of panel a in the region of V=O stretching vibrations; (c) 0.1 MLV, frequency region of oxide vibrations; and (d) close-up of panel c in the region of Al_2O_3 and Al–O–V vibrations. Of the three spectra displayed in each of the four panels, the top spectrum represents just a copy of the corresponding spectrum in Figure 3b; i.e., these spectra are referenced to the clean vanadia particles. The other two spectra are referenced to clean NiAl (— clean vanadia particles and (...) CO-saturated particles; consequently, dividing the dotted curve by the solid curve would lead again to the topmost spectrum).

In regard to the low-coverage preparation (0.1 MLV), the anti-peak observed there, at 1026 cm^{-1} , can readily be understood in terms of the interaction between V=O and CO. (Note that the V=O frequency is dependent on the vanadium coverage. As shown previously,³ the V=O frequency shifts to higher values, as a function of the increasing vanadium coverage.) The interesting frequency region in this experiment is located at $\sim 900 \text{ cm}^{-1}$, where the interface-localized Al–O–V vibrations are known to develop. However, at a vanadium coverage of only 0.1 MLV, the interface mode has not yet gained enough intensity to be unambiguously identified in the IR spectra. Instead, the spectra are still dominated by the presence of alumina substrate phonons (Figure 4c). For the uncovered alumina film kept at 90 K, these vibrations are found²⁷ at 871 and at 954 cm^{-1} . Upon CO adsorption on the vanadia-covered alumina, these bands remain basically unperturbed. However, some changes are visible in the region of $\sim 900 \text{ cm}^{-1}$, as evidenced by the close-up in Figure 4d. It is important to note, in this context, that previous CO adsorption experiments on rhodium, palladium, and iridium particles grown on the same support have revealed that the alumina phonons are influenced by adsorbed CO.²⁷ In these cases, clear changes of the absorption maxima at ~ 871 and $\sim 954 \text{ cm}^{-1}$ have been observed. They were attributed to changes in the metallicity of the adsorbing metal particles, which, in turn, influenced the alumina phonons. However, no modifications in the region between these phonons have been detected. Therefore, it is likely

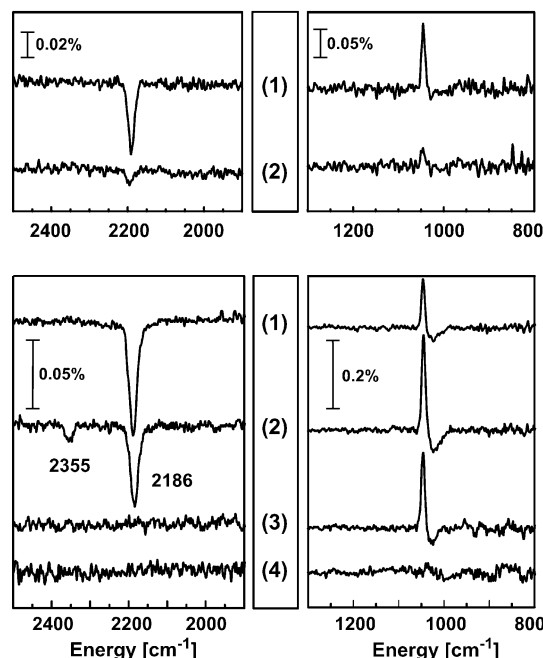


Figure 5. Sets of IR spectra of vanadia particles prepared by the evaporation of ~ 0.9 MLV. Experimental conditions are as in Figure 1. Upper panel: (1) after exposure to 0.1 L of CO and (2) after heating to 140 K. Lower panel: (1) after CO saturation, (2) after exposure to LEED electrons (100 eV, 30 min), (3) after heating to 200 K, and (4) after exposure to 0.5 L of O_2 .

that the existence of the anti-peak observed in Figure 3b is correlated to the Al—O—V interface species that are characteristic of our vanadia system. This idea is confirmed by recent CO adsorption experiments on vanadia particles of very similar properties which were grown on top of a silica thin-film support. There, neither an interface-localized oxide vibration nor an anti-peak signal, such as the one under discussion could be observed.²⁸ In contrast to that, such an anti-peak was also observed when CO was adsorbed on small vanadium particles that were deposited onto the alumina film under UHV conditions.²⁹ From previous investigations, we know that small amounts of vanadium are oxidized as they are deposited onto the alumina film.^{29,30} Obviously, this strong interaction between vanadium and the alumina film will lead to a modified interface region also in this case.

Interestingly, the appearance of a second anti-peak in the 0.1 MLV preparation coincides with the presence of the CO species P0 at ~ 2180 cm^{-1} . Both features are only observed in the low-coverage regime. The other anti-peak, on the contrary, is present over the entire coverage range, in analogy to the P1 species. Unfortunately, we did not succeed in providing further experimental evidence for a correlation between the CO species and the anti-peaks, because all these features develop in a parallel manner, both as a function of CO exposure and as a function of sample temperature.

3.3. CO Reaction. After having studied the low-temperature adsorption of CO on our alumina-supported particles, we have investigated their reactivity with respect to CO. In a first set of experiments, this was done by heating the sample and monitoring changes in the IR spectra. In the top panel of Figure 5, the corresponding result for a high-coverage preparation (0.9 MLV) is shown. Starting from CO-covered particles (spectrum (1), ~ 0.1 L of CO), the sample was heated from 90 K to a temperature of ~ 140 K, where the intensity due to CO stretching vibrations had completely vanished. To have a proper baseline, the sample was subsequently cooled back to 90 K, where the

IR spectrum labeled (2) in Figure 5 was taken. This procedure results in the recovery of a 100% line, i.e., the clean vanadia particles. (Note that there is some intensity at the CO position and the corresponding anti-peak position, because of CO that had been readsorbed during the last cooling step.) Now, exposing the particles a second time to ~ 0.1 L of CO leads back to spectrum (1). From this reversibility, we can conclude that CO desorbs from our vanadia particles molecularly, i.e., without dissociation or reaction to CO_2 . Indeed, if one of these processes had taken place, the spectra would have shown an irreversible behavior in the oxide vibration region either due to atomic carbon left on the surface or due to oxygen vacancies that are generated there. An example for such an irreversibility will be discussed in the following.

Regarding the reactivity properties of our system, the above-described investigations reveal that there is no thermal channel accessible for the oxidation of CO. To check whether the process can be activated nonthermally, in a second set of experiments, CO-saturated vanadia particles were exposed to low-energy electrons. This can either be done by directly supplying them via the electron gun of a LEED system or, for example, by exposing the sample to X-rays, thus producing photoelectrons. Such an experiment is presented in the lower portion of Figure 5. Spectrum (1) is taken from CO-saturated vanadia particles (0.9 MLV) at 90 K. After these particles were exposed at this temperature to LEED electrons with an energy of 100 eV for ~ 30 min, spectrum (2) was measured. In addition to a decrease in the CO intensity, a new species can be identified in the spectrum at 2355 cm^{-1} , which can be assigned to the asymmetric stretching vibration of a linear CO_2 species. In the oxide vibration region, an increase of the V=O-derived anti-peak can be noticed. It is important to note in this context that no carbonate or carboxylate species were observed. In addition, exposing the clean particles directly to CO_2 also renders just a linearly adsorbed species at the same frequency of 2355 cm^{-1} . Spectrum (3) shows the situation after desorption of the carbon oxide species and after subsequent cooling back to the reference temperature of 90 K. In contrast to what was shown in the top portion of Figure 5, the situation now is not reversible anymore; i.e., CO and CO_2 have completely disappeared from the spectrum but the anti-peak is still there, although somehow diminished with respect to the previous step.

There are two different conceivable reaction mechanisms that could explain the findings: (a) a Boudouard type of mechanism, where two CO molecules join to form CO_2 , leaving atomic carbon on the surface, and (b) a redox or Mars van-Krevelen type of mechanism, where lattice oxygen is transferred to the adsorbed CO molecule to form a CO_2 species. In both cases, the surface would have been altered irreversibly. To decide between these two mechanisms, the surface was exposed to molecular oxygen at 90 K. Evidently, an exposure of just 0.5 L of O_2 was sufficient to recover the 100% line, as shown in spectrum (4). Because there is no indication of newly formed CO, we conclude that the reaction proceeds via a redox mechanism. A definite proof, however, would require a preparation of our vanadia particles utilizing the oxygen isotope ^{18}O . Mechanism (b) then should lead to a lower CO_2 stretching frequency, whereas in the case of mechanism (a), a frequency of ~ 2355 cm^{-1} would be expected again.

To check whether the observed irreversibility could also be a direct consequence of the exposure to LEED electrons, we have performed a corresponding set of experiments, using clean, adsorbate-free vanadia particles. Indeed, irradiating the sample

with electrons that have an energy of 100 eV and for ~ 30 min did not lead to any changes.

Another important aspect is, of course, the question how the observed CO oxidation is dependent on the particle size. To answer this question, we have performed a corresponding set of experiments in the range of medium and high vanadium coverages: 0.24, 0.4, 0.9, and 1.8 MLV. In all these cases, the resulting CO₂ species exhibited a frequency and an integrated intensity that was comparable to the signal shown in Figure 5. Considering the higher number of adsorbed CO molecules in the case of the medium-coverage preparations, this means that the fraction of CO molecules that is converted to CO₂ is highest in the case of the high-coverage preparations. Another interesting observation is that the number of CO₂ molecules produced on a 0.9 MLV sample increased considerably (by a factor of ~ 2) when the particles were not saturated with CO prior to the oxidation step but just exposed to approximately one-third of the saturation dose.

4. Discussion

Following the presentation of the experimental results, their interpretation shall be discussed in this section, regarding, for example, the observed particle-size-dependent adsorption properties, the influence of the vanadia–alumina interface, and the role of vanadyl groups. The section is organized using the same format as that used in section 3.

4.1. CO Adsorption. The most conspicuous result of our CO adsorption experiments is the observed dependence on vanadium coverage. Particles that consist of ~ 25 V atoms per particle (0.3 MLV) are capable of adsorbing a maximum amount of CO molecules. In the low- and medium-coverage range, several different CO species are detected, whereas, for larger particles, only one adsorption site (P1) is present. The frequency and width of this dominating P1 species are strongly dependent on coverage. The same is true for the interaction between V=O groups on the particle surface and adsorbed CO molecules, which is strongest for medium-sized particles. At low coverages, CO was found to even influence Al–O–V interface vibrations.

How can these coverage dependences be explained? First, it must be emphasized that all the previously listed peculiarities are observed in the low- to medium-coverage region. From our previous structure investigations, we know that vanadia and alumina strongly interact with each other. It was shown that vanadia particles are partially incorporated into the alumina film and that the structure of the film becomes considerably distorted upon vanadia particle growth, accompanied by an increase in the thickness of the alumina film. Interestingly, the most drastic changes, such as the onset of alumina film growth, the disappearance of the alumina LEED pattern and the alumina phonons, as well as the appearance of Al–O–V vibrations occur in the same coverage regime (~ 0.2 – 0.4 MLV). It is quite unlikely that this is just a coincidence; rather, this indicates that the vanadia–alumina interface has a decisive role in our system, in regard to not only structural properties but also adsorption properties. The appearance of a second anti-peak at low coverages can be regarded as direct evidence for this idea of a mutual influence.

Further support comes from the observation that the frequencies of the P2 and P3 species, which exist only in the low- to medium-coverage range, are red-shifted with respect to the gas-phase value, indicating that they are not due to regular terrace sites. Instead, defect sites are likely to be involved, which are, at higher coverages, either not present or not accessible anymore. One example for defects which could lead to a red-shifted CO

frequency are oxygen vacancies (color centers). Theoretical calculations on MgO,³¹ for example, predict a transfer of negative charge to a CO molecule adsorbed on an oxygen vacancy; also, recent calculations on V₂O₅(010) single-crystal surfaces³² suggest the same phenomenon. However, there is no simple explanation why these defects should not exist anymore at higher vanadium coverages. A type of defect that could explain the findings under discussion more easily is a special kind of impurity. One example that has been discussed in the literature³¹ is that of Ni²⁺ ions replacing Mg²⁺ ions in MgO. There, a non-negligible π -back-donation from Ni²⁺ to CO was observed (in contrast to the case of Ni²⁺ in NiO). Given the strong interaction between the vanadia particles and the alumina support—partial incorporation, Al–O–V interface vibrations—similar defects are to be expected in our system also, i.e., V³⁺ ions replacing Al³⁺ ions in Al₂O₃. (Note that, as shown in previous experiments,²⁰ CO adsorbs on the clean alumina film only at temperatures < 60 K and at a frequency of 2172 cm^{-1} .) Another type of defect that frequently has an important role for the adsorption and reaction behavior of particle systems involves low-coordination sites (steps and corners). On alumina-supported rhodium particles, for example, it was found that particles that consist of ~ 100 – 200 Rh atoms are capable of dissociating a maximum amount of adsorbed CO. This could be explained on the basis of a particle-size-dependent number of steps on the particles.¹⁹ However, a corresponding particle size effect does not seem to apply for the system under discussion, because CO adsorbed on low-coordination sites should exhibit a frequency that is even further blue-shifted, as evidenced by calculations³³ and experiments.¹⁰

In conclusion, special conditions present at the vanadia–alumina interface are the most likely explanation for the observed particle size dependence in the CO adsorption behavior. To supply further evidence, we are currently studying vanadia particles of very similar structural and electronic properties that have been grown on top of a silica thin-film support.²⁸ For this system, a significantly reduced particle–support interaction was observed. Preliminary CO adsorption experiments on a 0.74 MLV preparation rendered a CO species that was similar to the P1 species at a frequency of 2198 cm^{-1} . At a medium coverage of 0.2 MLV, however, no extra peaks and no frequency shift of the P1-like species were detected, thus corroborating the idea of an adsorption behavior, which is less influenced by the interface.

4.2. Interaction of CO with Oxide Vibrations. A well-known phenomenon in surface science is the fact that adsorbed molecules are able to interact with each other. The most intensively studied case is probably that of CO molecules adsorbed on metal surfaces where a CO-coverage-dependent blue-shift of the IR signals is observed. This frequency shift essentially consists of two different contributions: a chemical contribution and a vibrational contribution.¹⁸ The chemical shift can be understood on the basis of the Blyholder model, i.e., with an increasing competition for π -back-donation electrons as a function of CO coverage. The vibrational shift is caused by dipole–dipole interactions, i.e., by the coupling of dipoles with the oscillating electric field produced by neighboring dipoles. However, the corresponding dipoles must have very similar frequencies to achieve an efficient coupling. In the present case of interaction between CO stretching vibrations and oxide vibrations (V=O and Al–O–V), this condition is definitely not fulfilled, so a dynamic coupling mechanism can be excluded from consideration. Alternatively, static dipole interactions (the Stark effect) might have a role. In this case,

the vibration frequency of an adsorbed molecule is influenced by the presence of an electric field that can be applied either externally (cf. CO/Ni(110)^{34,35}) or which can be produced by neighboring dipoles (cf. CO coadsorption experiments³⁶). The resulting frequency shift of an adsorbed dipole is dependent on its orientation, relative to the electric field with which it interacts: a parallel orientation leads to a red-shift, whereas an antiparallel orientation leads to a blue-shift.³⁷ Note that, in the case where two different dipoles interact with each other, the frequencies of both of them are shifted in the same direction. However, as shown in section 3.2 for the interaction between CO and V=O, this does not seem to apply for the system under discussion, in marked contrast to the assumption that static dipole interactions are the dominant mechanism. Instead, an indirect interaction via modifications in the local electronic structure that are induced by CO (and V=O) is more likely.

4.3. CO Oxidation. Vanadia-based catalysts are generally applied in the partial oxidation of hydrocarbons; therefore, only a few studies on the oxidation of CO to CO₂ are available in the literature.^{25,38,39} According to these studies, CO can be oxidized thermally on both alumina-supported and polycrystalline vanadia.²⁵ In the latter case, CO oxidation has already occurred at temperatures as low as 170 K, where an intense band that is centered at 2340 cm⁻¹ and has a shoulder at 2355 cm⁻¹ was found in the IR spectra. The authors proposed V⁵⁺ centers to be responsible for the oxidation reaction. Consequently, it is maybe not too surprising that our vanadia particles—being characterized by an average oxidation state of +3—exhibit such a low reactivity. Indeed, hydrogen and hydrocarbon oxidation experiments on thin, well-ordered V₂O₃ films revealed that oxygen removal from vanadium oxide becomes more difficult as the oxide is reduced.⁴⁰ However, according to a recent theoretical study on the interaction of CO with an ideal, V=O-terminated V₂O₅(010) single crystal, a completely oxidized surface that exhibits only V⁵⁺ centers is also unreactive.³² Calculations for the energy barrier regarding a reaction between CO and the differently coordinated O atoms present in V₂O₅ rendered comparatively high values of up to 2 eV. Consequently, desorption is the process that is predicted upon heating. Interestingly, an excitation of the V₂O₅ surface via a highest occupied molecular orbital—lowest unoccupied molecular orbital (HOMO—LUMO) transfer of electrons from O 2p into V 3d orbitals resulted in a considerably reduced reaction barrier on the order of ~1 eV. Experimentally, such an excitation could be achieved, for example, by an irradiation of the surface with low-energy electrons or with X-rays. In analogy to the previously presented results, this should lead to the formation of CO₂ also in the case of a V₂O₅(010) surface.

Because the vanadia particles investigated in this study are, in accordance with technical catalysts, terminated with V=O groups, we can use our experiments to examine the role of vanadyl groups during oxidation reactions, which is an issue that has been under debate for quite a long time.^{1,2} To elucidate what is happening to the V=O groups on our sample, we must reference the spectra presented in Figure 5 to the clean NiAl. The result is displayed in Figure 6, where a close-up of the corresponding spectra in the region of V=O stretching frequencies is shown. In addition to spectra (1)–(4), we have also added a spectrum labeled (0), which represents the situation before CO adsorption, i.e., for the clean vanadia particles. Comparing spectrum (0) and spectrum (2), one could come to the conclusion that the V=O groups are indeed consumed during the reaction, because the corresponding peak intensity has considerably decreased. However, the V=O intensity had already decreased

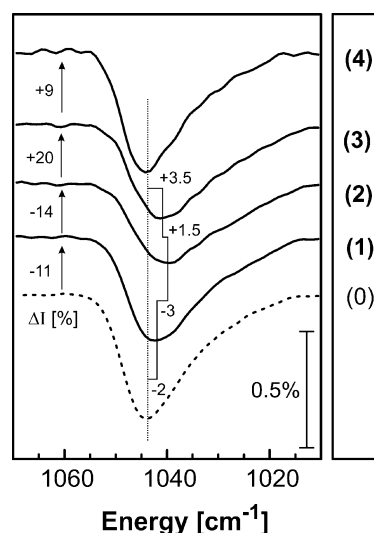


Figure 6. Spectra (1)–(4) are those presented in the lower panel of Figure 5 but are now referenced to clean NiAl. In addition, a corresponding spectrum for the clean, uncovered vanadia particles is shown (spectrum (0)). Frequency and intensity changes are both indicated in the graphic; the values given there refer to the corresponding changes, with respect to the previous spectrum, as one follows the development from spectrum (0) to spectrum (4). The frequency change is given in units of cm⁻¹, and the intensity change ΔI is given as a percentage, according to the following example: $\Delta I(1,0) = (I_1 - I_0)/I_0$.

just upon CO adsorption, where no consumption of the vanadyl oxygen is expected. Finally, the fact that the V=O intensity grows again upon desorption of CO and CO₂ is definitely in conflict with the idea of vanadyl oxygen being consumed. We therefore suggest that the observed intensity and frequency changes are only due to the interaction between adsorbates and V=O groups, possibly mediated via modifications of the electronic structure in the vicinity of the adsorption site, which leads to changes in the V=O bond length and in the orientation of the V=O bond axis. In conclusion, it is more probable that the V=O groups on our vanadia particles are just spectator species that are not directly involved in the reaction process. Instead, bridging V–O species are more likely to deliver the active oxygen. This might explain also why the fraction of CO molecules converted to CO₂ is highest in the case of the high-coverage preparations, where a larger number of bridging V–O species should be available, in comparison to the medium-coverage preparations. Unfortunately, we could not identify a corresponding V–O species in the coverage regime under discussion (<2 MLV), revealing that their dynamic dipole moment is either too small to be detected in the IR spectra or must be oriented essentially parallel to the NiAl substrate.

5. Summary and Conclusion

Utilizing infrared (IR) spectroscopy, we have studied the interaction of carbon monoxide (CO) molecules with a model catalyst system that is composed of vanadia particles deposited onto a thin-film alumina support grown on NiAl (110). Combining the results of these studies with our previous investigations³ regarding the structural characterization of the system by means of scanning tunneling microscopy (STM), X-ray photoelectron spectroscopy (XPS), and IR spectroscopy, we have arrived at the following conclusions.

Low-temperature CO adsorption leads to a very complex behavior, as a function of vanadia particle size. For large particles, only one CO species is observed, which is shown to

interact with vanadyl groups (V=O) present at the surface of the particles. At lower vanadium coverages, however, the CO adsorbates seem to become increasingly influenced by the presence of the alumina–vanadia interface, resulting in a red-shifted stretching frequency. In addition to that, three further CO species are detected on the smaller particles, the existence of which is most likely correlated to the presence of defects and to the interaction with the interface. Generally, the alumina–vanadia interface has a decisive role in regard to the adsorption behavior. This is evidenced, for example, by an additional, interface-related feature present in the IR spectra of low-coverage preparations but also by the observation that particles in the medium-coverage regime are capable of adsorbing a maximum amount of CO. In summary, the most intensive interaction with adsorbed CO occurs in a regime where the alumina support is covered with a large number of densely packed, small vanadia particles.

The reactivity of our model system was quite limited, as thermal treatment resulted only in a molecular desorption of CO. Nevertheless, an oxidation reaction could be induced by means of low-energy electrons that are supplied either by an electron gun or by exposing the sample to X-rays. The interaction between the CO molecules and the V=O groups evidently is a helpful way to provide information about the processes on the surface. The results suggest that CO oxidation on our alumina-supported vanadia particles proceeds via a redox, i.e., a Mars–van Krevelen mechanism. The vanadyl oxygen, however, does not seem to be the active oxygen. Instead, bridging V–O species are more likely to supply the active oxygen.

Acknowledgment. The authors gratefully acknowledge financial support by the Deutsche Forschungsgemeinschaft (DFG) through the Sonderforschungsbereich 546 and by the Athena consortium. N.M. thanks the Studienstiftung des deutschen Volkes for a fellowship. J.B.G. and A.H. thank the Natural Sciences and Engineering Research Council of Canada and the Deutscher Akademischer Austauschdienst (DAAD), respectively. Finally, we are grateful to Ch. Friedrich, M. Frank, and M. Naschitzki for their various helpful contributions.

References and Notes

- (1) Bond, G. C.; Tahir, S. F. *Appl. Catal.* **1991**, *71*, 1.
- (2) Deo, G.; Wachs, I. E.; Haber, J. *Crit. Rev. Surf. Chem.* **1994**, *4*, 141.
- (3) Magg, N.; Giorgi, J. B.; Schroeder, T.; Bäumer, M.; Freund, H.-J. *J. Phys. Chem. B* **2002**, *106*, 8756.
- (4) Jaeger, R. M.; Kühlenbeck, H.; Freund, H.-J.; Wuttig, M.; Hoffmann, W.; Franchy, R.; Ibach, H. *Surf. Sci.* **1991**, *259*, 235.
- (5) Bäumer, M.; Freund, H.-J. *Prog. Surf. Sci.* **1999**, *61*, 127.
- (6) Stierle, A.; Renner, F.; Streitl, R.; Dosch, H. *Phys. Rev. B* **2001**, *64*, 165413.
- (7) Note that, from our previous STM measurements,³ we can calculate from the vanadia coverage (expressed in terms of the number of monolayers of vanadium, MLV) the average number of V atoms per particle, which is often a more meaningful quantity, to characterize the particle size. Of course, the vanadia particles additionally contain a certain number of O atoms whose exact value is not known but which can be estimated on the basis of our XPS analysis to be ~1.5 times greater than the number of V atoms.)
- (8) Schönnenbeck, M.; Cappus, D.; Klinkmann, J.; Freund, H.-J.; Pettersson, L. G. M.; Bagus, P. S. *Surf. Sci.* **1996**, *347*, 337.
- (9) Vesceky, S. M.; Xu, X.; Goodman, D. W. *J. Vac. Sci. Technol. A* **1994**, *12*, 2114.
- (10) Zaki, M. I.; Knözinger, H. *J. Catal.* **1989**, *119*, 311.
- (11) Escalona Platero, E.; Coluccia, S.; Zecchina, A. *Surf. Sci.* **1986**, *171*, 465.
- (12) Davydov, A. A. *Infrared Spectroscopy of Adsorbed Species on the Surface of Transition Metal Oxides*; Wiley: New York.
- (13) Pacchioni, G.; Cogliandro, G.; Bagus, P. S. *Surf. Sci.* **1991**, *255*, 344.
- (14) Dupuis, A.-C. Thesis, Humboldt Universität Berlin, Germany, 2002.
- (15) Dupuis, A.-C.; Kühlenbeck, H.; Freund, H.-J., to be published.
- (16) Concepcion, P.; Reddy, B. M.; Knözinger, H. *Phys. Chem. Chem. Phys.* **1999**, *1*, 3031.
- (17) Jonson, B.; Rebenstorf, B.; Larsson, R.; Andersson, S. L. T.; Lundin, S. T. *J. Chem. Soc., Faraday Trans. 1* **1986**, *82*, 767.
- (18) Hoffmann, F. M. *Surf. Sci. Rep.* **1983**, *3*, 107.
- (19) Frank, M.; Bäumer, M. *Phys. Chem. Chem. Phys.* **2000**, *2*, 3723.
- (20) Frank, M. Thesis, Humboldt Universität Berlin, Germany, 2000. (In Ger.)
- (21) Lauterbach, J.; Boyle, R. W.; Schick, M.; Mitchell, W. J.; Meng, B.; Weinberg, W. H. *Surf. Sci.* **1996**, *350*, 32.
- (22) Seiferth, Thesis, O. Ruhr-Universität Bochum, 1997. (In Ger.)
- (23) Pykavy, M.; Staemmler, V.; Seiferth, O.; Freund, H.-J. *Surf. Sci.* **2001**, *479*, 11.
- (24) Note that, in IR spectroscopy, it is convenient to measure relative changes instead of absolute signals, to eliminate contributions from the spectrometer setup (light source, beam splitter, mirrors, etc.). This is done by dividing two single-channel spectra by each other (sample spectrum/reference spectrum). In the present case, the intensity reflected from CO-saturated vanadia particles (sample spectrum) was divided by the intensity reflected from the clean particles (reference spectrum).
- (25) Busca, G.; Ramis, G.; Lorenzelli, V. *J. Mol. Catal.* **1989**, *50*, 231.
- (26) Miyata, H.; Kohno, M.; Ono, T.; Ohno, T.; Hatayama, F. *J. Mol. Catal.* **1990**, *63*, 181.
- (27) Frank, M.; Wolter, K.; Magg, N.; Heemeier, M.; Kühnemuth, R.; Bäumer, M.; Freund, H.-J. *Surf. Sci.* **2001**, *492*, 270.
- (28) Magg, N.; Immaraporn, B.; Giorgi, J. B.; Schroeder, T.; Bäumer, M.; Freund, H.-J., manuscript in preparation.
- (29) Magg, N.; Giorgi, J. B.; Frank, M.; Schroeder, T.; Bäumer, M.; Freund, H.-J., manuscript in preparation.
- (30) Bäumer, M.; Biener, J.; Madix, R. J. *Surf. Sci.* **1999**, *432*, 189.
- (31) Pacchioni, G. *Surf. Rev. Lett.* **2000**, *7*, 277.
- (32) Friedrich, Ch.; Hermann, K., manuscript in preparation.
- (33) Pacchioni, G.; Minerva, T.; Bagus, P. S. *Surf. Sci.* **1992**, *275*, 450.
- (34) Lambert, D. K. *Phys. Rev. Lett.* **1983**, *50*, 2106.
- (35) Bagus, P. S.; Nelin, C. J.; Müller, W.; Philpott, M. R.; Seki, H. *Phys. Rev. Lett.* **1987**, *58*, 559.
- (36) Mate, C. M.; Kao, C.-T.; Somorjai, G. A. *Surf. Sci.* **1988**, *206*, 145.
- (37) Griffin, G. L.; Yates, J. T., Jr. *J. Chem. Phys.* **1982**, *77*, 3744.
- (38) Roozeboom, F.; van Dillen, A. J.; Geus, J. W.; Gellings, P. J. *Ind. Eng. Chem. Prod. Res. Dev.*, **1981**, *20*, 304.
- (39) Ruitenbeek, M.; van Dillen, A. J.; de Groot, F. M. F.; Wachs, I. E.; Geus, J. W.; Koningsberger, D. C. *Top. Catal.* **2000**, *10*, 241.
- (40) Lewis, K. B.; Oyama, S. T.; Somorjai, G. A. *Surf. Sci.* **1990**, *233*, 75.